Anatomic and Flow Characteristics of Left Anterior Descending Coronary Artery Angiographic Stenoses Predisposing to Myocardial Infarction

Demosthenes G. Katritsis, MD, PhD[a,*], Ioannis Pantos, PhD[a], Theodoros Zografos, MD, PhD[a], Aferdita Spahillari, MD[b], Antoinette de Waha, MD[c], Anastasios Kopanidis, PhD[a], Stephanos Foussas, MD[a], Peter H. Stone, MD[d], Adnan Kastrati, MD[c], and Donald Cutlip, MD[e]

The impact of the anatomic characteristics of coronary stenoses on the development of future coronary thrombosis has been controversial. This study aimed at identifying the anatomic and flow characteristics of left anterior descending (LAD) coronary artery stenoses that predispose to myocardial infarction, by examining angiograms obtained before the index event. We identified 90 patients with anterior ST-elevation myocardial infarction (STEMI) for whom coronary angiograms and their reconstruction in the three-dimensional space were available at 6 to 12 months before the STEMI, and at the revascularization procedure. The majority of culprit lesions responsible for STEMI occurred between 20 and 40 mm from the LAD ostium, whereas the majority of stable lesions not associated with STEMI were found in distances >60 mm ($p < 0.001$). Culprit lesions were significantly more stenosed (diameter stenosis 68.6 ± 14.2% vs 44.0 ± 10.4%, $p < 0.001$), and significantly longer than stable ones (15.3 ± 5.4 mm vs 9.2 ± 2.5 mm, $p < 0.001$). Bifurcations at culprit lesions were significantly more frequent (88.8%) compared with stable lesions (34.4%, $p < 0.001$). Computational fluid dynamics simulations demonstrated that hemodynamic conditions in the vicinity of culprit lesions promote coronary thrombosis due to flow recirculation. A multiple logistic regression model with diameter stenosis, lesion length, distance from the LAD ostium, distance from bifurcation, and lesion symmetry, showed excellent accuracy in predicting the development of a culprit lesion (AUC: 0.993 [95% CI: 0.969 to 1.000], $p < 0.0001$). In conclusion, specific anatomic and hemodynamic characteristics of LAD stenoses identified on coronary angiograms may assist risk stratification of patients by predicting sites of future myocardial infarction. © 2020 Published by Elsevier Inc. **(Am J Cardiol 2021;141:7−15)**

The impact of coronary stenosis severity on the development of plaque rupture and thrombosis, and subsequent myocardial infarction (MI), has been controversial. MIs have been shown to frequently occur at sites of mild-to-moderate stenosis.[1−3] Postmortem and older angiographic data, however, have demonstrated that ruptured plaques leading to thrombosis more likely occur within the segment of complex lesions with significant (>50%) stenoses.[4−8] Apart from lesion severity, the anatomical distribution and characteristics of coronary segments prone to thrombosis and subsequent MI in the coronary tree, have also been studied. Angiography,[9] intravascular ultrasound,[10] computed tomography,[11] and pathology[12] studies have demonstrated that culprit lesions are not uniformly distributed at the coronary tree, but rather tend to cluster at specific anatomic regions. We have previously reported on the anatomic relationships of the site of culprit lesions that resulted in acute ST-elevation myocardial infarction (STEMI) on three-dimensional (3D) reconstructed angiograms,[13] and have also compared the anatomic characteristics of recanalized left anterior descending (LAD) arteries following an anterior MI with stable lesions identified in the LAD of the same patient.[14] However, these results were limited by the fact that only recanalized LADs that were analyzed after the STEMI, could be studied. Furthermore, culprit and stable lesions were derived from different patients; therefore, pathophysiology background may not have been similar.

In the current serial angiographic study on coronary angiograms that were available at 6 to 12 months before, and at the time of, and at the time of the acute event, we sought to study the anatomic and hemodynamic characteristics of coronary stenoses that evolve to culprit lesions leading to MI versus those that remain stable, in the same patient. We also analysed reconstructed LAD 3D models of patients with STEMI-related culprit lesions and stable lesions, and employed computational fluid dynamics (CFD) simulations for assessment of hemodynamic conditions which predispose to development of occlusive thrombus formation.[15] To the best of our knowledge, this is the first human study to conduct such an analysis on coronary angiograms obtained before and after an acute thrombotic event.

[a]Hygeia Hospital, Athens, Greece; [b]Massachusetts General Hospital, Harvard Medical School, Boston, Massachusetts; [c]Deutsches Herzzentrum, München, Germany; [d]Brigham and Women's Hospital, Harvard Medical School, Boston, Massachusetts; and [e]Beth Israel Deaconess Medical Center, Harvard Medical School, Boston, Massachusetts. Manuscript received September 28, 2020; revised manuscript received and accepted November 9, 2020.

There is no conflict of interest for any author to be declared.

*Corresponding author: Tel: +306944845505

E-mail address: dkatrits@dgkatritsis.gr (D.G. Katritsis).

0002-9149/© 2020 Published by Elsevier Inc.
https://doi.org/10.1016/j.amjcard.2020.11.012

Methods

We identified 90 patients from three Cardiology Departments with anterior STEMI and coronary angiograms available both at 6 to 12 months before revascularization (first angiogram), and at the revascularization procedure (second angiogram) (Table 1). STEMI was defined according to the third universal definition of the Joint ESC/ACCF/AHA/WHF task force. In each angiogram we identified the culprit lesions associated with the STEMI, and stable lesions at the LAD which had not evolved into thrombosis. The patient population was randomly divided into a derivation cohort of 61 patients with 200 lesions available for analysis and a validation cohort of 29 patients with 95 lesions available for analysis. The study was ethically approved by our institutional review boards.

The lesion responsible for STEMI was defined as the culprit lesion at first angiogram. Detectable (before or after recanalization, and regardless of diameter % stenosis) lesions on the LAD that did not evolve to MI between the first and second angiogram, were considered as stable lesions. Each culprit lesion of an individual patient was compared with every other stable lesion that was identified in the LAD of the same patient.

Three-dimensional reconstruction was accomplished with the use of a reconstruction algorithm developed by our group.[16,17] Angiograms were analysed by the same investigators in the study core laboratory (Coronary Flow Research Unit at Hygeia Hospital, Athens). From the 3D model of the reconstructed coronary tree, the following features were extracted for each lesion: (1) the distance from the ostium of LAD to the point of minimal luminal diameter within the lesion, (2) the lesion length, considered as the distance from the proximal to the distal lesion point not affected by atherosclerosis, (3) the number of side branches with orifices on the lesion before the site of minimal luminal diameter, and the number of side branches with orifices on the lesion after the site of minimal luminal diameter, (4) the distance of the lesion from side branches measured in respect to the point of minimal luminal diameter within the lesion, (5) The local curvature of the LAD at the site of the lesion which was measured selecting 3 points on the 3D model, 1 at the apex of the observed curvature and the other 2 at noncurved parts of the vessel proximal and distal to the lesion. Local curvature was defined as the angle specified by these points with the angle apex set on the stenosis, (6) the position of the lesion in respect to the local vessel curvature. This was assessed by identifying whether the lesion resided in the inner or the outer vessel wall in respect to the local vessel curvature. In the cases that both vessel walls were affected by atherosclerosis, the lesion was characterized as "symmetrical". Thus, the position of each lesion was characterized as "in," "out," or "symmetrical".

The execution of CFD simulations require the vessel model which is recreated as a 3D digital model, and the Navier-Stokes equations that describe the laminar or turbulent motion of fluids are numerically solved using numerical grids.[15,18]

The normality of continuous variables was assessed by the Shapiro-Wilk test. Continuous variables are presented as mean value ± standard deviation, and categorical variables as absolute (n) and relative frequencies (%). Association between the type of lesion (i.e., culprit or stable) and continuous variables were evaluated using Student's *t* test, and Mann-Whitney test when continuous variables were normally distributed and skewed, respectively. The association between categorical variables was evaluated through chi-square test without the correction of continuity. The predictive (or discriminating) ability of the anatomic lesion characteristics and the proposed index in predicting culprit lesions compared with stable ones was assessed by using the area under the receiver operating characteristic (ROC) curve (AUC). The optimal cut-off value for each anatomic characteristic and the proposed lesion score was determined with the estimation of its corresponding Youden index. Multiple logistic regression analysis was performed including the anatomic characteristics that were found to be significantly associated with the type of lesion (i.e., culprit or stable) in the univariate analysis as independent categorical variables, according to the determined optimal cut-off values, and the type of lesion as dependent variable. A scoring system was developed by rounding the values of the coefficients of the multiple logistic regression model to the nearest integer. Finally, univariate logistic regression was used to calculate the predicted probability of evolution to culprit lesion based on the proposed score. A 2-sided p-value <0.05 was considered statistically significant. All ROC curve analyses were performed with MedCalc Statistical Software version 14.8.1 (MedCalcSoftware bvba, Ostend, Belgium). All other statistical calculations were performed using IBM SPSS Statistics, version 23.0 (IBM Corp., Armonk, New York).

Table 1
Clinical characteristics of patients

	Total (n = 90)
Age (years)	57.4 ± 11.3
Men	76 (84%)
Diabetes Mellitus	18 (20%)
Hypertension	57 (63%)
Hypercholesterolemia	69 (77%)
Family history of coronary artery disease	30 (33%)
Smoker	32 (36%)
Interval between 1st − 2nd angiogram (months)	7.2±4.1
Culprit/stable lesions per patient	1(n = 90) / 2.3 ± 0.8 (n = 205)

Results

Table 1 presents clinical characteristics of patients who were studied. The derivation cohort consisted of 61 patients with 61 culprit lesions and 139 stable lesions, whereas the validation cohort consisted of 29 patients with 29 culprit and 66 stable lesions.

Table 2 illustrates the anatomic characteristics and relationships of culprit and stable lesions.

Culprit lesions were significantly more stenosed than stable ones at the first angiogram (Table 2 and Figure 1). Lesion length was greater in culprit than stable lesions at the first angiogram (Table 2). The ROC curve analysis revealed that the discriminating ability of diameter stenosis

Table 2
LAD anatomic characteristics of culprit and stable lesions in the 1st angiogram

Anatomic parameter	Culprit lesions (n = 90)	Stable lesions (n = 205)	p
% diameter stenosis	68.6 ± 14.2	45.7 ± 11.2	<0.001
Distance from the ostium (mm)	33.3 ± 13.3	66.8 ± 20.3	<0.001
Lesion length (mm)	15.3 ± 5.4	9.2 ± 2.5	<0.001
LAD reference diameter (mm)	3.0 ± 0.4	2.4 ± 0.4	0.020
Bifurcation on-lesion (y/n)			
No bifurcation on-lesion	10 (11.2%)	134 (65.6%)	
Before the point of max stenosis	20 (22.5%)	32 (15.5%)	
After the point of max stenosis	27 (30.2%)	25 (12.1%)	<0.001
Both before and after the point of max stenosis	33 (36.1%)	14 (6.9%)	
Distance of lesion from side branch	9.6 ± 7.4mm	15.3 ± 4.4mm	0.02
Lesion position in respect to local curvature			
In	22 (24.2%)	63 (30.8%)	0.08
Out	24 (26.2%)	62 (30.2%)	0.10
Symmetrical	44 (49.6%)	80 (39.0%)	0.02
Lesion curvature in diastole in 3D (degrees)	160.8 ± 13.9	170.9 ± 10.7	0.01

to predict a lesion evolving into a culprit lesion was high (AUC: 0.933 [95% CI: 0.888 to 0.964), p < 0.0001). The cut-off point analysis showed that diameter stenosis >55% constitutes the optimal threshold to discriminate between stable lesions and lesions evolving into culprit lesions (sensitivity: 83.61% and specificity: 93.28%). According to ROC curve analysis, lesion length had moderate discriminating ability to identify lesions evolving into culprit (AUC:0.862 [95% CI: 0.807 to 0.907], p < 0.0001). A cut-off value of lesion length >10.4 mm was identified as the optimal threshold to discriminate between stable lesions and lesions evolving into culprit with a sensitivity of 81.97% and a specificity of 79.86%.

The distance of the lesion from the ostium of the LAD was statistically significantly longer in stable lesions compared with culprit lesions (Table 2 and Figure 2). According to ROC curve analysis, distance from LAD ostium had high discriminating ability to identify lesions evolving into culprit (AUC:0.912 [95% CI: 0.864 to 0.948], p < 0.0001). The cut-off point analysis showed that distance from LAD ostium ≤49 mm constitutes an optimal threshold to discriminate between stable lesions and lesions evolving into culprit lesions (sensitivity: 90.16% and specificity: 80.43%).

According to ROC curve analysis, distance between the lesion and a bifurcation proximal to the lesion as well as distance between the lesion and a bifurcation distal to the

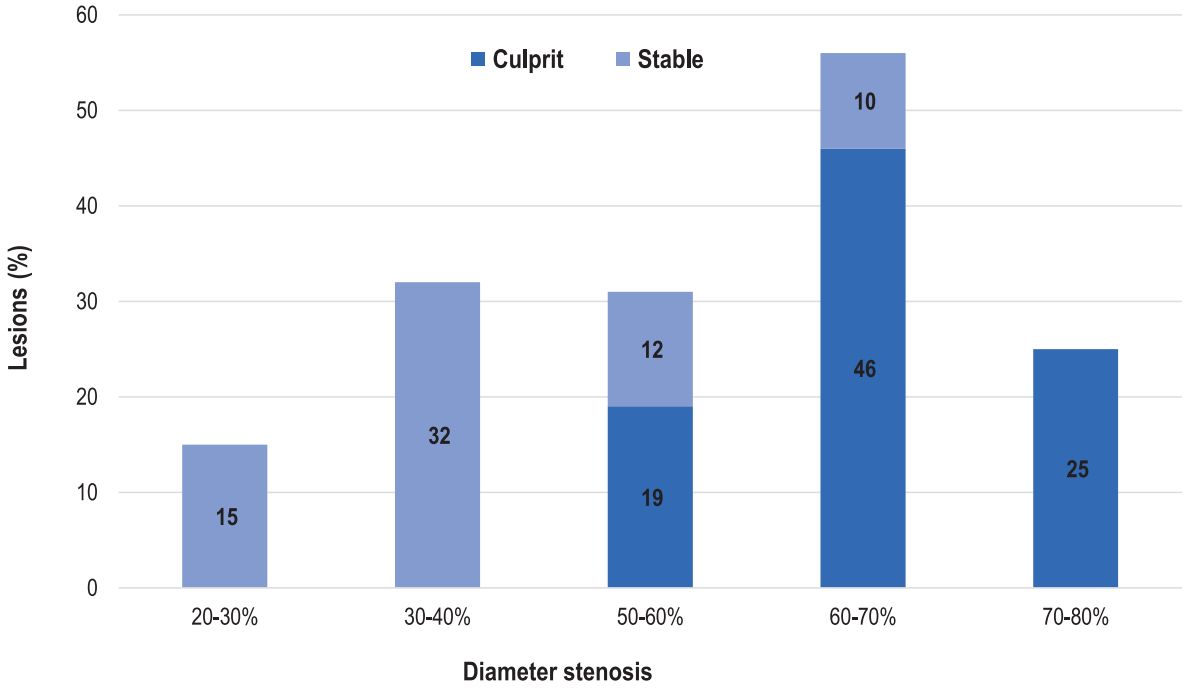

Figure 1. Distribution of % diameter stenosis for culprit (1st angiogram) and stable lesions.

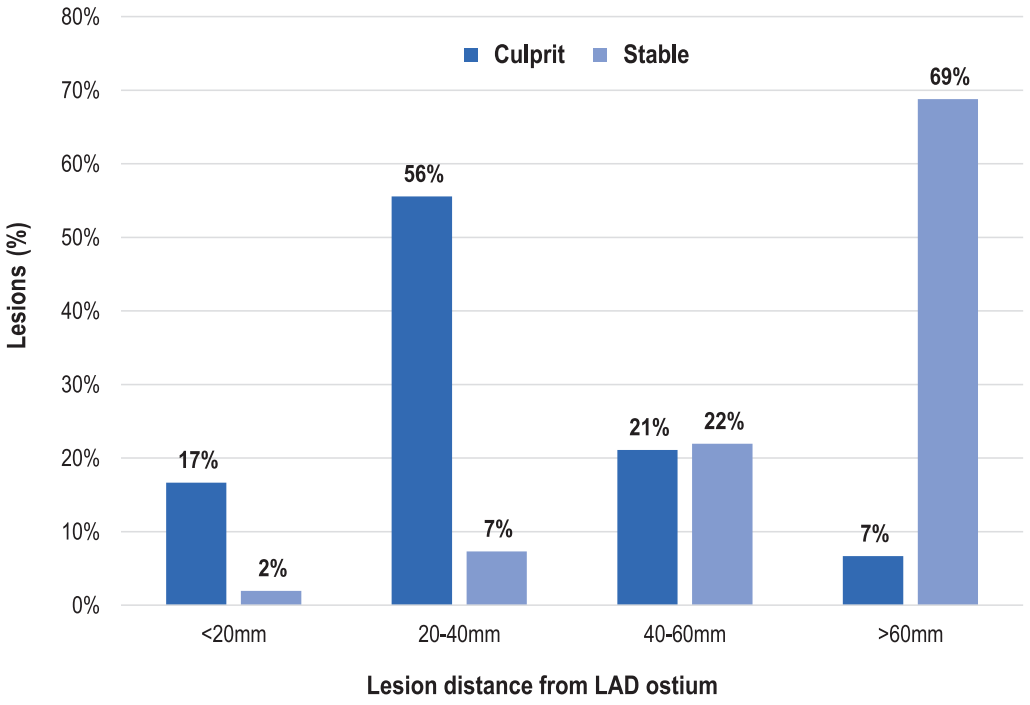

Figure 2. Lesion distribution along the LAD.

lesion have moderate discriminatory ability to identify lesions evolving into culprit (AUC: 0.797 [95% CI: 0.734 to 0.850], $p < 0.0001$; AUC:0.806 [95% CI: 0.745 to 0.859], $p < 0.0001$; respectively).

There was no statistically significant difference in the frequency that culprit and stable lesions resided at the inner or outer vessel wall in respect to the local vessel curvature. However, culprit lesions were more frequently symmetrical than stable lesions, that is, affecting both aspects of the vessel wall (Table 2). Vessel angulation at the lesion site was significantly sharper in culprit lesions as compared with stable ones (Table 2), but according to ROC curve analysis, vessel angulation had moderate discriminatory ability to identify lesions evolving into culprit (AUC: 0.720 [95% CI: 0.647 to 0.786], $p < 0.0001$).

Using the above-mentioned cut-off values, we constructed a multiple logistic regression model with diameter stenosis, lesion length, distance from the LAD ostium, distance from bifurcation, lesion symmetry, and vessel angulation included as independent categorical variables. All variables, except vessel angulation, were independently associated with the presence of a lesion identified as the culprit lesion in the second angiogram (Table 3). Using ROC curve analysis, the resulting model incorporating diameter stenosis, lesion length, distance from the LAD ostium, distance from bifurcation, and lesion symmetry, showed excellent accuracy in predicting the development of a culprit lesion (AUC: 0.993 [95% CI: 0.969 to 1.000], $p < 0.0001$). According to their regression coefficients, each anatomic characteristic was assigned with a weight corresponding to specific points and the sum of all assigned points is used to calculate a lesion specific score ranging from 2 to 21 (Table 3). The resulting lesion score had high predictive ability in the derivation cohort, identical to the full model (AUC:0.993 [95% CI :0.968 to 1.000], $p < 0.0001$). In cut-off analysis, the optimal threshold to discriminate lesions evolving into culprit in the second angiogram is a lesion score >10, with a sensitivity of 96.72% and a specificity of 95.49%) (Figure 3). In the validation cohort, the AUC of the proposed lesion score was 0.992 (95% CI: 0.947 to 1.000). Using the >10 cut-off value, the lesion score in the validation cohort achieved a sensitivity of 100% and a

Table 3
Multivariate logistic regression model for lesion evolution into a culprit lesion according to anatomic characteristics

	Multivariate analysis			Assigned points per predictor variable
Predictor variable	OR	95%CI	p Value	
Diameter Stenosis ≥55%	98.79	11.18-873.22	<0.0001	5
Lesion length ≥10.4 mm	62.83	6.27-629.17	<0.0001	4
Distance from Ostium ≤49 mm	111.03	10.31-1195.95	<0.0001	5
Proximity to Bifurcation*	105.01	1.83-6012.08	0.024	5
Symmetrical lesion	11.15	1.50-82.95	0.019	2

Lesion score calculation: Score is calculated by adding the assigned points for each one of the five anatomic characteristics.
* Distance ≤12.5 mm between the lesion and a bifurcation proximal to the lesion or ≤9.9mm between the lesion and a bifurcation distal to the lesion.

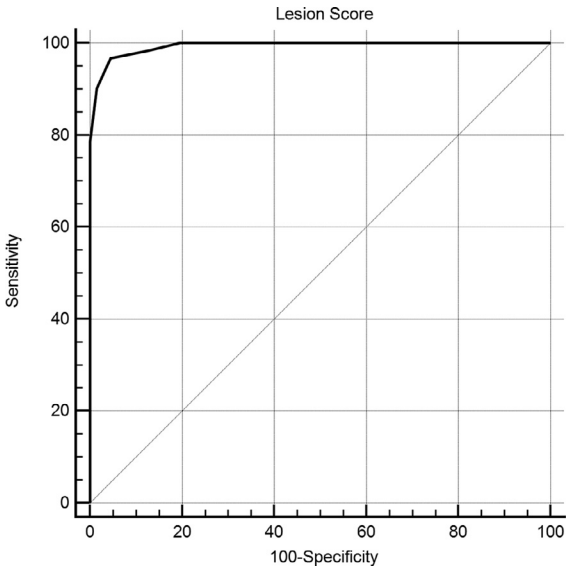

Figure 3. Receiver operating characteristic curve of the diagnostic ability of the proposed lesion score for the detection of a lesion evolving into culprit.

specificity of 85.07%. The predicted probabilities for the evolution into a culprit lesion in the second angiogram according to our proposed lesion score are presented in Figure 4.

Table 4
Progression of stable lesions between the 1st and 2nd angiogram

	Anatomic parameter			
	% diameter stenosis	p	Lesion length (mm)	p
1st angiogram (n = 201)	44.0 ± 10.4	0.09	9.2 ± 2.5	0.2
2nd angiogram (n = 205)	45.7 ± 11.2		9.5 ± 2.4	

The total number of stable lesions did not change significantly with time since only in 4 patients (2.2%) new lesions were detected, and all new lesions caused mild arterial constriction (<30%) (Table 4).

Based on the analysis of the anatomic features of culprit and stable coronary lesions, we derived the coronary segments associated with MI and stable lesions, and reconstructed these segments as vessel models with lesions of percent diameter stenosis of 50% and 90% that represented borderline and definitively significant disease. We studied flow distribution, and particularly flow recirculation and vortex formation at the vicinity of the lesion (Figures 5 and 6). Figure 5 shows that in the culprit lesion model, a 50% diameter stenosis induces flow recirculation at the orifice of

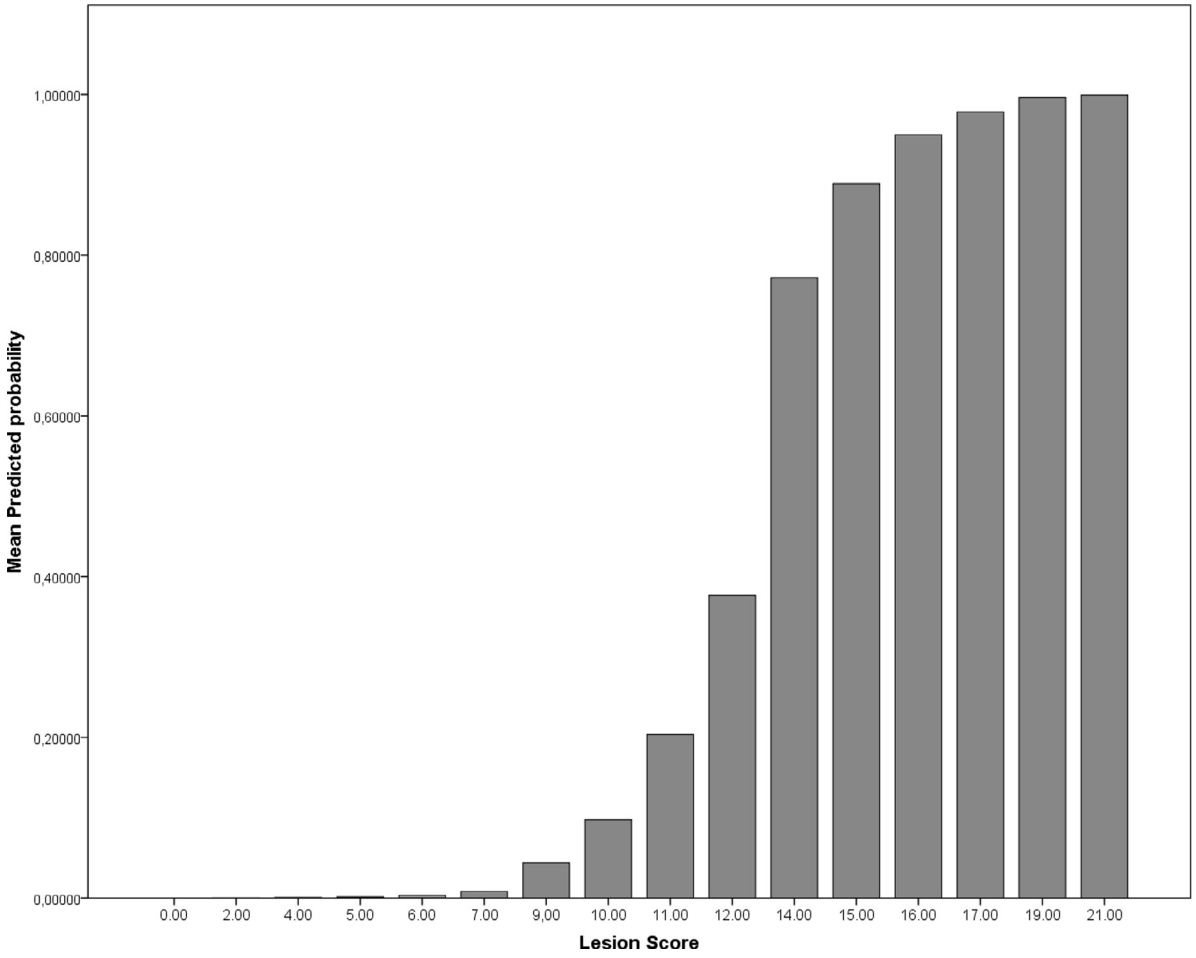

Figure 4. Predicted probabilities for the evolution into a culprit lesion in the second angiogram according to our proposed lesion score.

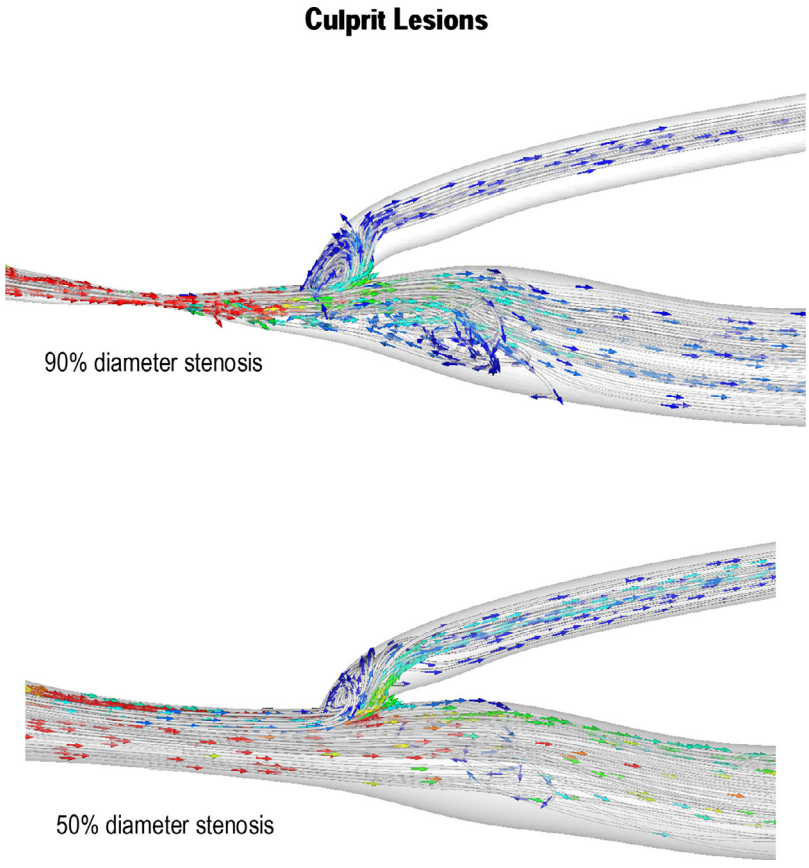

Figure 5. Flow distribution in the culprit lesion model with 90% and 50% diameter stenosis.

the poststenotic side branch. Restricting the flow downstream of the bifurcation point results in the formation of a strong recirculation zone at the ostium of the side branch. Such vortex formation is not present in the stable lesion model (Figure 6). Analysis of the flow lines over the whole cardiac cycle indicates that for most of the cardiac cycle, the flow is not significantly affected. This is fundamentally different from the flow distribution developing within the culprit lesion model. Figure 5 shows that for a severe (90%) stenosis in the culprit lesion model flow is practically blocked not only to the poststenotic branch, but also just downstream of the stenosis along the main branch. The 90% stenosis causes severe flow recirculation not only in the culprit lesion model but also in the poststenotic lumen of the stable lesion model (Figure 6). For the quantification of flow recirculation and deviations in cases we also investigated the temporal variation of area blockage percentage of each branch for all considered models.

Discussion

Our data indicate that specific anatomic and fluid dynamics characteristics are associated with subsequent coronary occlusion and increase the potential of a coronary lesion to result in an acute coronary event. Thus, detailed examination of coronary anatomy and associated hemodynamic characteristics are useful both for defining the extent of atherosclerotic disease, as well as for predicting the risk of individual lesions to result in a future infarction.

The prognostic significance of the severity of individual lesions has been a matter of controversy. In the PROSPECT trial on patients with acute coronary syndromes treated by coronary intervention, 3-year recurrence rates were 20%. Half of them occurred in angiographically mild (<70% stenosis), nonculprit lesions. However, predictors of recurrent events were both a luminal area ≤ 4 mm^2, and the presence of thin-cap fibroatheroma.[19] In the SCOT-HEART trial, low-attenuation plaque was the strongest predictor of fatal or nonfatal MI, exceeding other markers such as coronary artery stenosis.[3] Our results indicate that coronary thrombosis is more likely to occur at coronary lesions with significant rather than low diameter % stenosis. These observations are in keeping with data from other contemporary studies. An analysis of the data of the COURAGE trial has also shown that MIs are not likely to occur from mild coronary lesions compared with moderate or severe ones; the number of non-revascularized lesions >=50% was the only angiographic predictor or an acute coronary syndrome.[20] In the ROMICAT trials, lesions with >=50% stenosis were detected in 78% of patients with ACS.[21] Data from a large retrospective cohort study of patients undergoing elective coronary angiography, have also demonstrated that obstructive (stenoses>=70%) CAD were associated with worse outcomes such as MI and death. Patients with nonobstructive CAD were at increased risk compared with those with no apparent CAD.[8] The recent International Study of Comparative Health Effectiveness With Medical and Invasive Approaches (ISCHEMIA) trial provides clear evidence that the extent of CAD is associated with

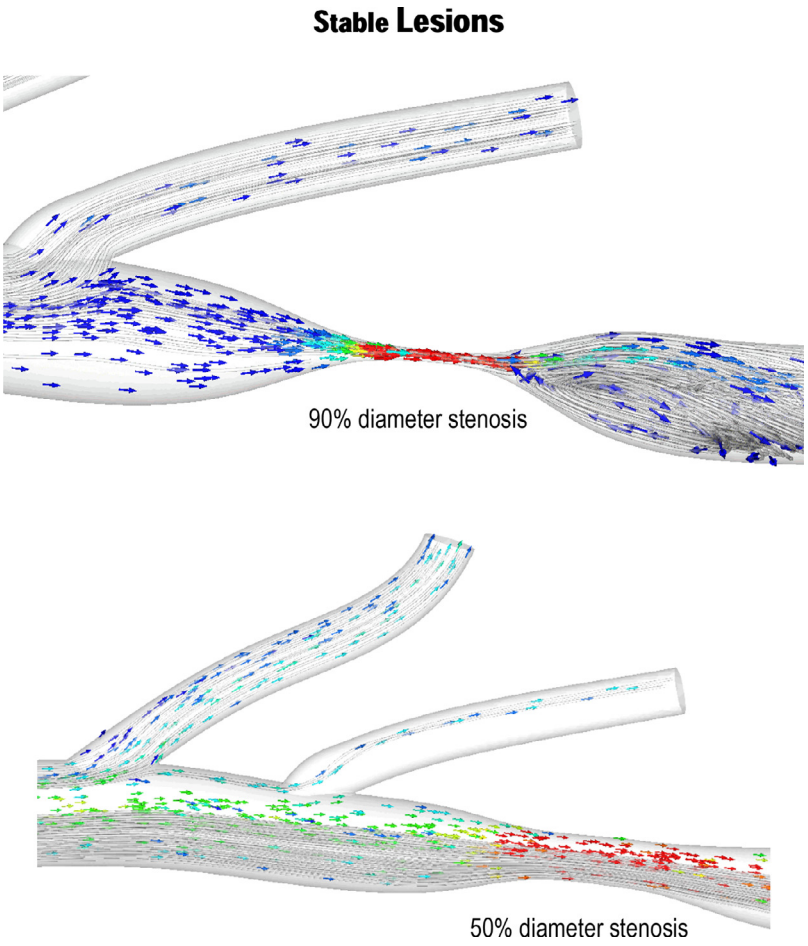

Figure 6. Flow distribution in the stable lesion model with 90% and 50% diameter stenosis.

increased incidence of adverse cardiac events, but that the severe flow-limiting coronary stenoses are not the responsible culprit site.[2] Our results add evidence to indicate that significant coronary stenoses constitute an important risk factor for the development of MI, and the associated CFD characteristics provide the rationale for this effect. The strength of our study represents the first human study to conduct such a comprehensive assessment of the evolution of coronary lesions leading to an acute STEMI in the same patient.

Lesion distribution and vulnerability have been associated with the distribution of wall shear stress (WSS), along the coronary tree.[22] Arterial regions exposed to low time-averaged WSS, or to patterns of shear stress that change direction, seem prone to atherosclerosis, whereas regions exposed to shear stress with higher magnitude and uniform direction are protected.[23] Previous studies showed that low WSS regions occur at bifurcations in regions opposite the flow dividers and also low shear stress values appear in the proximal regions of the LAD if there is a local branch or tortuosity there or up- or down-stream from a focal obstruction.[22] In keeping with these findings, our data suggest that culprit lesions are more frequently located close to side branches and at the proximal regions of LAD. Additionally, the distance from the coronary ostium has been identified as an independent determinant of lipid content, with lesions located at the proximal coronary segments being associated with higher lipid content and plaque vulnerability.[24] The presence of bifurcations also denotes an increased risk of plaque rupture and, more importantly, subsequent thrombosis. Bifurcations have also been associated with the potential for ruptured plaques.[10,13] Very high shear stress does not predispose to atheroma formation, but may promote plaque rupture.[14] A highly localized circumferential wall stress concentration of approximately 9 to 14 times the proximal circumferential wall stress occurs at bifurcation sites,[25] which, in addition, undergo a larger deformation during cyclic flexion of the coronary artery, yielding a higher circumferential stress.[26]

Plaque formation at a particular coronary site and its subsequent rupture may not necessarily lead to ACS.[27,28] Multiple plaque ruptures remote from the culprit lesion in patients with ACS have been demonstrated, and plaque ruptures have also been identified in patients with stable angina or asymptomatic ischemia.[28] Therefore, not all ruptured plaques have the same potential for subsequent thrombosis and development of MI. Fluid dynamics parameters also appear to play a significant role in this process. Pulsating flow conditions as those of coronary circulation result in oscillatory and vorticity-stream flow patterns at sites of bifurcations, with demonstration of back-flow in the presence of even minimal atherosclerosis.[29] The development of recirculation zones might facilitate the accumulation of

blood thrombogenic factors close to the wall,[30] and thus favour occlusive thrombus formation following plaque rupture.

A limitation of our study is that lesions that did not form a thrombosis between the first and second angiogram for a time interval of 7.2 ± 4.1months were considered stable, but we cannot confirm their stability over a longer period of time. However, even during this time the difference in the evolution of culprit vs stable lesions was remarkable. Second, conventional angiograms used in this study do not provide as precise detail of coronary artery wall and plaque borders as the gold-standard invasive imaging (OCT and IVUS), and the 3D lumen reconstruction and CFD analysis may not be as accurate as invasive imaging. The 3D reconstruction methods force the lumen to be a circle, and this forced geometry loses much of the critical micro geometry that results from an eccentric and heterogeneous plaque protruding into the lumen. Still, detected flow patterns provided the rationale for observed angiographic and clinical outcomes. Finally, we have not used intravascular ultrasound or optical coherence tomography to assess additional parameters of lesion histology that could affect the possibility of plaque rupture and thrombosis. Our study is based on purely conventional angiography which, however, still represents the most often used imaging variety in catheter labs worldwide.

In conclusion, our data indicate that not all coronary plaques evolve equally in the same patient. Specific anatomic and hemodynamic characteristics of LAD segments and stenoses associated with STEMI can be identified on coronary angiograms and assist the risk stratification of patients by means of predicting potential sites of producing MI.

1. Giroud D, Li JM, Urban P, Meier B, Rutishauer W. Relation of the site of acute myocardial infarction to the most severe coronary arterial stenosis at prior angiography. *Am J Cardiol* 1992;69:729–732.
2. Maron DJ, Hochman JS, Reynolds HR, Bangalore S, O'Brien SM, Boden WE, Chaitman BR, Senior R, Lopez-Sendon J, Alexander KP, Lopes RD, Shaw LJ, Berger JS, Newman JD, Sidhu MS, Goodman SG, Ruzyllo W, Gosselin G, Maggioni AP, White HD, Bhargava B, Min JK, Mancini GBJ, Berman DS, Picard MH, Kwong RY, Ali ZA, Mark DB, Spertus JA, Krishnan MN, Elghamaz A, Moorthy N, Hueb WA, Demkow M, Mavromatis K, Bockeria O, Peteiro J, Miller TD, Szwed H, Doerr R, Keltai M, Selvanayagam JB, Steg PG, Held C, Kohsaka S, Mavromichalis S, Kirby R, Jeffries NO, Harrell FE Jr., Rockhold FW, Broderick S, Ferguson TB Jr., Williams DO, Harrington RA, Stone GW, Rosenberg Y, Group IR. Initial invasive or conservative strategy for stable coronary disease. *N Engl J Med* 2020;382:1395–1407.
3. Williams MC, Kwiecinski J, Doris M, McElhinney P, D'Souza MS, Cadet S, Adamson PD, Moss AJ, Alam S, Hunter A, Shah ASV, Mills NL, Pawade T, Wang C, Weir McCall J, Bonnici-Mallia M, Murrills C, Roditi G, van Beek EJR, Shaw LJ, Nicol ED, Berman DS, Slomka PJ, Newby DE, Dweck MR, Dey D. Low-attenuation noncalcified plaque on coronary computed tomography angiography predicts myocardial infarction: results from the multicenter SCOT-HEART trial (scottish computed tomography of the HEART). *Circulation* 2020;141:1452–1462.
4. Finn AV, Nakano M, Narula J, Kolodgie FD, Virmani R. Concept of vulnerable/unstable plaque. *Arterioscler Thromb Vasc Biol* 2010;30:1282–1292.
5. Qiao JH, Fishbein MC. The severity of coronary atherosclerosis at sites of plaque rupture with occlusive thrombosis. *J Am Coll Cardiol* 1991;17:1138–1142.
6. Kaski JC, Chester MR, Chen L, Katritsis D. Rapid angiographic progression of coronary artery disease in patients with angina pectoris. The role of complex stenosis morphology. *Circulation* 1995;92:2058–2065.
7. Ojio S, Takatsu H, Tanaka T, Ueno K, Yokoya K, Matsubara T, Suzuki T, Watanabe S, Morita N, Kawasaki M, Nagano T, Nishio I, Sakai K, Nishigaki K, Takemura G, Noda T, Minatoguchi S, Fujiwara H. Considerable time from the onset of plaque rupture and/or thrombi until the onset of acute myocardial infarction in humans: coronary angiographic findings within 1 week before the onset of infarction. *Circulation* 2000;102:2063–2069.
8. Maddox TM, Stanislawski MA, Grunwald GK, Bradley SM, Ho PM, Tsai TT, Patel MR, Sandhu A, Valle J, Magid DJ, Leon B, Bhatt DL, Fihn SD, Rumsfeld JS. Nonobstructive coronary artery disease and risk of myocardial infarction. *JAMA* 2014;312:1754–1763.
9. Katritsis DG, Efstathopoulos EP, Pantos J, Korovesis S, Kourlaba G, Kazantzidis S, Marmarelis V, Voridis E. Anatomic characteristics of culprit sites in acute coronary syndromes. *J Interv Cardiol* 2008;21:140–150.
10. Hong MK, Mintz GS, Lee CW, Lee BK, Yang TH, Kim YH, Song JM, Han KH, Kang DH, Cheong SS, Song JK, Kim JJ, Park SW, Park SJ. The site of plaque rupture in native coronary arteries: a three-vessel intravascular ultrasound analysis. *J Am Coll Cardiol* 2005;46:261–265.
11. Hoffmann U, Moselewski F, Nieman K, Jang IK, Ferencik M, Rahman AM, Cury RC, Abbara S, Joneidi-Jafari H, Achenbach S, Brady TJ. Noninvasive assessment of plaque morphology and composition in culprit and stable lesions in acute coronary syndrome and stable lesions in stable angina by multidetector computed tomography. *J Am Coll Cardiol* 2006;47:1655–1662.
12. Cheruvu PK, Finn AV, Gardner C, Caplan J, Goldstein J, Stone GW, Virmani R, Muller JE. Frequency and distribution of thin-cap fibroatheroma and ruptured plaques in human coronary arteries: a pathologic study. *J Am Coll Cardiol* 2007;50:940–949.
13. Katritsis DG, Pantos I, Korovesis S, Hadjipavlou M, Tzanalaridou E, Lockie T, Redwood S, Voridis E, Efstathopoulos EP. Three-dimensional analysis of vulnerable segments in the left anterior descending artery. *Coron Artery Dis* 2009;20:199–206.
14. Katritsis DG, Efstathopoulos EP, Pantos I, Tzanalaridou E, De Waha A, Siontis GC, Toutouzas K, Redwood S, Kastrati A, Stefanadis C. Ruptured versus stable plaques in human coronary arteries. *Coron Artery Dis* 2011;22:345–351.
15. Katritsis DG, Theodorakakos A, Pantos I, Andriotis A, Efstathopoulos EP, Siontis G, Karcanias N, Redwood S, Gavaises M. Vortex formation and recirculation zones in left anterior descending artery stenoses: computational fluid dynamics analysis. *Phys Med Biol* 2010;55:1395–1411.
16. Katritsis DG, Pantos I, Efstathopoulos EP, Tzanalaridou E, Korovesis S, Kourlaba G, Paxinos G, Voridis E. Three-dimensional analysis of the left anterior descending coronary artery: comparison with conventional coronary angiograms. *Coron Artery Dis* 2008;19:265–270.
17. Andriotis A, Zifan A, Gavaises M, Liatsis P, Pantos I, Theodorakakos A, Efstathopoulos EP, Katritsis D. A new method of three-dimensional coronary artery reconstruction from X-ray angiography: validation against a virtual phantom and multislice computed tomography. *Catheter Cardiovasc Interv* 2008;71:28–43.
18. Katritsis D, Kaiktsis L, Chaniotis A, Pantos J, Efstathopoulos EP, Marmarelis V. Wall shear stress: theoretical considerations and methods of measurement. *Prog Cardiovasc Dis* 2007;49:307–329.
19. Stone GW, Maehara A, Lansky AJ, de Bruyne B, Cristea E, Mintz GS, Mehran R, McPherson J, Farhat N, Marso SP, Parise H, Templin B, White R, Zhang Z, Serruys PW. A prospective natural-history study of coronary atherosclerosis. *N Engl J Med* 2011;364:226–235.
20. Mancini GB, Hartigan PM, Bates ER, Sedlis SP, Maron DJ, Spertus JA, Berman DS, Kostuk WJ, Shaw LJ, Weintraub WS, Teo KK, Dada M, Chaitman BR, O'Rourke RA, Boden WE. Angiographic disease progression and residual risk of cardiovascular events while on optimal medical therapy: observations from the COURAGE Trial. *Circ Cardiovasc Interv* 2011;4:545–552.
21. Puchner SB, Liu T, Mayrhofer T, Truong QA, Lee H, Fleg JL, Nagurney JT, Udelson JE, Hoffmann U, Ferencik M. High-risk plaque detected on coronary CT angiography predicts acute coronary syndromes independent of significant stenosis in acute chest pain: results from the ROMICAT-II trial. *J Am Coll Cardiol* 2014;64:684–692.
22. Eshtehardi P, McDaniel MC, Suo J, Dhawan SS, Timmins LH, Binongo JN, Golub LJ, Corban MT, Finn AV, Oshinski JN, Quyyumi

AA, Giddens DP, Samady H. Association of coronary wall shear stress with atherosclerotic plaque burden, composition, and distribution in patients with coronary artery disease. *J Am Heart Assoc* 2012;1: e002543.
23. Peiffer V, Sherwin SJ, Weinberg PD. Does low and oscillatory wall shear stress correlate spatially with early atherosclerosis? A systematic review. *Cardiovasc Res* 2013;99:242–250.
24. Valgimigli M, Rodriguez-Granillo GA, Garcia-Garcia HM, Malagutti P, Regar E, de Jaegere P, de Feyter P, Serruys PW. Distance from the ostium as an independent determinant of coronary plaque composition in vivo: an intravascular ultrasound study based radiofrequency data analysis in humans. *Eur Heart J* 2006;27:655–663.
25. Salzar RS, Thubrikar MJ, Eppink RT. Pressure-induced mechanical stress in the carotid artery bifurcation: a possible correlation to atherosclerosis. *J Biomech* 1995;28:1333–1340.
26. Wu HC, Chen SY, Shroff SG, Carroll JD. Stress analysis using anatomically realistic coronary tree. *Med Phys* 2003;30:2927–2936.
27. Hong MK, Mintz GS, Lee CW, Kim YH, Lee SW, Song JM, Han KH, Kang DH, Song JK, Kim JJ, Park SW, Park SJ. Comparison of coronary plaque rupture between stable angina and acute myocardial infarction: a three-vessel intravascular ultrasound study in 235 patients. *Circulation* 2004;110:928–933.
28. Maehara A, Mintz GS, Bui AB, Walter OR, Castagna MT, Canos D, Pichard AD, Satler LF, Waksman R, Suddath WO, Laird JR Jr., Kent KM, Weissman NJ. Morphologic and angiographic features of coronary plaque rupture detected by intravascular ultrasound. *J Am Coll Cardiol* 2002;40:904–910.
29. Chakravarty S, Sen S. Analysis of pulsatile blood flow in constricted bifurcated arteries with vorticity-stream function approach. *J Med Eng Technol* 2008;32:10–22.
30. Feldman CL, Ilegbusi OJ, Hu Z, Nesto R, Waxman S, Stone PH. Determination of in vivo velocity and endothelial shear stress patterns with phasic flow in human coronary arteries: a methodology to predict progression of coronary atherosclerosis. *Am Heart J* 2002;143:931–939.